



1

1 **Carbonate System Parameters of an Algal-dominated Reef along West Maui**

2

3 Nancy G. Prouty<sup>1</sup>, Kimberly K. Yates<sup>2</sup>, Nathan Smiley<sup>2</sup>, Chris Gallagher<sup>3</sup>, Olivia Cheriton<sup>1</sup>, and Curt  
4 D. Storlazzi<sup>1</sup>

5

6 <sup>1</sup>U.S. Geological Survey, Coastal and Marine Geology, Pacific Coastal and Marine Science Center, Santa Cruz, CA 95060

7 <sup>2</sup>U.S. Geological Survey, Coastal and Marine Geology, St. Petersburg Coastal and Marine Science Center 600 4th Street  
8 South, St. Petersburg, FL 33701

9 <sup>3</sup>University of California, Santa Cruz, Santa Cruz, CA 95060

10

11 *Correspondence to:* Nancy G. Prouty [nprouty@usgs.gov](mailto:nprouty@usgs.gov)



## 12 **Abstract**

13 Constraining coral reef metabolism and carbon chemistry dynamics are fundamental for understanding  
14 and predicting reef vulnerability to rising coastal CO<sub>2</sub> concentrations and decreasing seawater pH.  
15 However, few studies exist along reefs occupying densely inhabited shorelines with known input from  
16 land-based sources of pollution. The shallow coral reefs off Kahekili, West Maui, are exposed to  
17 nutrient-enriched, low-pH submarine groundwater discharge (SGD) and are particularly vulnerable to  
18 the compounding stressors from land-based sources of pollution and lower seawater pH. To constrain  
19 the carbonate chemistry system, nutrients and carbonate chemistry were measured along the Kahekili  
20 reef flat every 4 h over a 6-d sampling period in March 2016. Abiotic process - primarily SGD fluxes -  
21 controlled the carbonate chemistry adjacent to the primary SGD vent site, with nutrient-laden  
22 freshwater decreasing pH levels and favoring undersaturated aragonite saturation ( $\Omega_{\text{arag}}$ ) conditions. In  
23 contrast, diurnal variability in the carbonate chemistry at other sites along the reef flat was driven by  
24 reef community metabolism. Superimposed on the diurnal signal was a transition during the second  
25 sampling period to a surplus of total alkalinity (TA) and dissolved inorganic carbon (DIC) compared to  
26 ocean end-member TA and DIC measurements. A shift from net community production and  
27 calcification to net respiration and carbonate dissolution was identified. This transition occurred during  
28 a period of increased SGD-driven nutrient loading, lower wave height, and reduced current speeds.  
29 This detailed study of carbon chemistry dynamics highlights the need to incorporate local effects of  
30 nearshore oceanographic processes into predictions of coral reef vulnerability and resilience.

31

## 32 **1. Introduction**

33 Coral reefs provide critical shoreline protection and important ecosystem services, such as marine  
34 habitat, and support local economies through tourism, fishing, and recreation ( Hughes et al., 2003;  
35 Ferrario et al., 2014). However, coral reefs are being threatened by global climate change processes,  
36 such as increasing temperatures, ocean acidification (OA), and sea-level rise, and these effects are  
37 often compounded by local stressors from over-fishing, sedimentation, coastal acidification, and land-  
38 based sources of pollution (Knowlton and Jackson, 2008). Isolating the effects of these stressors is  
39 difficult without establishing the biological and physical controls on community calcification and  
40 production. This is particularly challenging for coral reefs adjacent to densely inhabited shorelines,  
41 where freshwater fluxes can deliver excess nutrients, leading to eutrophication and coastal  
42 acidification, outbreaks of harmful algal blooms (Anderson et al., 2002), and decreased coral  
43 abundance and diversity (Fabricius, 2005; Lapointe et al., 2005). In many cases, eutrophication can  
44 alter ecosystem function and structure by shifting reefs from coral- to algae-dominated (Howarth et al.,



45 2000; Andrefouet et al., 2002; Hughes et al., 2007). Changes in community structure can have  
46 profound impacts on coral reef metabolism and reef carbon chemistry dynamics, which are ultimately  
47 linked to reef health, and the ability to predict future responses to rising  $p\text{CO}_2$  levels (Andersson and  
48 Gledhill, 2013). Understanding the local drivers of ecosystem function and reef community  
49 metabolism is critical for gauging the susceptibility of the reef ecosystem to future changes in ocean  
50 chemistry.

51

52 Numerous efforts have been conducted along west Maui, Hawaii, USA, to characterize and quantify  
53 submarine groundwater discharge (SGD) and associated nutrient input (Dailer et al., 2010; Dailer et al.,  
54 2012; Glenn et al., 2013; Swarzenski et al., 2013; Swarzenski et al., 2016). Until this study, however,  
55 no field-based measurements of carbonate system parameters were available from the reefs in this area.  
56 The carbonate chemistry system is sensitive to changes in photosynthesis, respiration, calcification,  
57 and dissolution, and can be characterized by measuring total alkalinity (TA), dissolved inorganic  
58 carbon (DIC), pH,  $p\text{CO}_2$ , nutrients, salinity, and temperature. Analysis of these parameters yields  
59 valuable information on ratios of net community calcification and production, and can be used to  
60 identify biological and physical drivers of reef health and ecosystem function (Silverman et al., 2007;  
61 Shamberger et al., 2011; Lantz et al., 2014; Albright et al., 2015; Muehllehner et al., 2016; DeCarlo et  
62 al., 2017). Here, we present high temporal-resolution, in-situ measurements of carbonate chemistry  
63 dynamics collected from the shallow coral reef off Kahekili in Kaanapali, west Maui, Hawaii, USA  
64 (Fig. 1), with the aim of assessing the environmental controls on carbon metabolism (photosynthesis  
65 and respiration, calcification and dissolution), and evaluating reef community performance and  
66 function. This is particularly important given growing concern that coastal and ocean acidification may  
67 shift reef ecosystems from net calcification to net dissolution by the mid to end of the century (  
68 Silverman et al., 2009; Andersson and Gledhill, 2013) with an overall reduction in calcification rates  
69 and increase in dissolution rates (Shamberger et al., 2011; Shaw et al., 2012; Bernstein et al., 2016)  
70 that can contribute to reef collapse (Yates et al., 2017).

71

72 The health of many of Maui's coral reefs has been declining rapidly (Rodgers et al., 2015), with recent  
73 coral bleaching events leading to increased coral mortality (Sparks et al., 2016). The decline in coral  
74 cover along the shallow coral reef at Kahekili has been observed for decades (Wiltse, 1996; Ross et al.,  
75 2012), along with a history of macro-algal blooms (Smith et al., 2005). The shift in benthic cover from  
76 abundant corals to turf- or macro-algae (primarily *Ulva fasciata*) and increased rates of coral  
77 bioerosion has been linked to input of nutrient-rich water via wastewater injection wells (Dailer et al.,



4

78 2010;Dailer et al., 2012; Prouty et al. 2017a). Treated wastewater is injected through these wells into  
79 groundwater that flows toward the coast where it emerges on the reef through a network of small seeps  
80 and vents (Glenn et al., 2013;Swarzenski et al., 2016). Changes in coastal water quality observed off  
81 west Maui can impact the balance of production of  $\text{CaCO}_3$  skeletons by plants and animals on the reef,  
82 cementation of sand and rubble, and  $\text{CaCO}_3$  breakdown and removal that occurs through bioerosion,  
83 dissolution, and offshore transport. Here, a high-resolution seawater sampling study was conducted to  
84 constrain the carbonate chemistry system and evaluate the biological and physical processes altering  
85 reef health along the shallow coral reef at Kahekili. This study represents the first characterization of  
86 diurnal and multi-day variability of coral reef carbonate chemistry along a tropical fringing reef  
87 adjacent to a densely inhabited shoreline with known input from land-based sources of pollution, and  
88 identifies the controls on carbon metabolism. Ultimately, understanding carbonate system dynamics is  
89 essential for managing compounding effects from local stressors.

90

## 91 **2. Methods**

### 92 *2.1 Study Site*

93 The benthic habitat along the shallow reef at Kahekili in Kaanapali, West Maui (Fig. 1) consists of  
94 aggregate reef, patch reef, pavement, reef rubble and spur and groove (Cochran et al., 2014), with  
95 persistent current flow to the south (Storlazzi and Jaffe, 2008). Only 51% of the hardbottom at  
96 Kahekili is covered with at least 10% live coral (Cochran et al., 2014). The shallow fore reef  
97 experiences algae blooms, in response to inputs of nutrient-rich water via wastewater injection wells  
98 (Dailer et al., 2010;Dailer et al., 2012). Groundwater inputs occur from both natural sources (rainfall  
99 and natural infiltration) and from artificial recharge (irrigation and anthropogenic wastewater). The  
100 inland Wailuku Basalt, consisting of a band of unconsolidated sediment along the coast, and a small  
101 outcrop of Lahaina Volcanics, dominates the geology of the area surrounding the study site, controlling  
102 the flow of groundwater. Mean annual precipitation rates are up to  $900 \text{ cm yr}^{-1}$  (Giambelluca et al.,  
103 2013), with natural recharge the greatest in the interior mountains.

104

### 105 *2.2 Field Sampling*

106 Two intensive sampling periods were carried out during the 6-d period between 16 to 24 March 2016.  
107 Seawater nutrients and carbonate chemistry variables were collected every 4 h during each sampling  
108 period from the primary vent site and in adjacent coastal waters along the shallow reef at Kahekili (Fig.  
109 1). The first sampling period was from 15:00 on 16 March 2016 to 15:00 on 19 March 2016, and the  
110 second sampling period was from 15:00 on 21 March 2016 to 11:00 on 24 March 2016 (all reported



111 times in local [HST]). There were five sampling sites: two shallow (<1.5 m) sites (S1 and S2) located  
112 approximately 10 m offshore, two deeper (5 m) sites (S3 and S4) located approximately 115 m  
113 offshore, and a shallow site located approximately 20 m offshore and adjacent to an active SGD vent  
114 (vent site) (Glenn et al., 2013; Swarzenski et al., 2016). Sampling tubes (ranging from approximately  
115 100 to 200 m in length) were installed at each site by affixing the tube to a concrete block located  
116 approximately 20 cm above the seafloor, or by attaching the tubing directly to dead reef structure using  
117 zip ties. Tube intakes were fitted with a stainless steel screen cap to prevent uptake of large  
118 particulates. The remaining length of each tube was positioned along the seafloor to the adjacent beach  
119 by weighting the tube with a 1 m piece of chain, or by weaving the tube through dead reef structure  
120 approximately every 20 m. The tube outflow ends were labeled for each sampling site, bundled in a  
121 common location, and located above the high water line on the beach for sampling access. A peristaltic  
122 pump was used to pump seawater from the seafloor. Sampling tubes were flushed for a minimum of 20  
123 minutes to remove residual seawater before collecting data and water samples. Temperature ( $\pm$   
124  $0.01^{\circ}\text{C}$ ), salinity ( $\pm 0.01$ ), and dissolved oxygen ( $\pm 0.1 \text{ mg L}^{-1}$ ) of water samples were measured using a  
125 YSI ProPlus multimeter that was calibrated daily. However, due to temperature change during water  
126 transit time within the sampling tube, in-situ temperatures were also recorded from Solonist CTD  
127 Divers installed at the intake of each sampling tube. An upward-looking 2-MHz Nortek Aquadopp  
128 acoustic Doppler profiler (ADP) was deployed at the southern deeper site (S4). The ADP sampled  
129 waves at 2 Hz for 17 min every hour and currents at 1 Hz every 10 min in 1-m vertical bins from 1 m  
130 above the seabed up to the ocean surface.

131

### 132 2.3 Seawater Analyses

133 Samples for dissolved nutrients ( $\text{NH}_4^+$ , Si,  $\text{PO}_4^{3-}$ , and  $[\text{NO}_3^- + \text{NO}_2^-]$ ) were collected in duplicate by  
134 filtering water with an in-line  $0.45\text{-}\mu\text{m}$  filter and  $0.20\text{-}\mu\text{m}$  syringe filter, and were kept frozen until  
135 analysis. Nutrients were analyzed at the Woods Hole Oceanographic Institution's nutrient laboratory  
136 and University of California at Santa Barbara's Marine Science Institute Analytical Laboratory via  
137 flow injection analysis for  $\text{NH}_4^+$ , Si,  $\text{PO}_4^{3-}$ , and  $[\text{NO}_3^- + \text{NO}_2^-]$ , with precisions of 0.6-3.0%, 0.6-0.8%,  
138 0.9-1.3%, and 0.3%-1.0% relative standard deviations, respectively. Select samples were collected and  
139 analyzed for nitrate isotope ( $\delta^{15}\text{N}$  and  $\delta^{18}\text{O}$ ) analyses at the University of California at Santa Cruz  
140 using the chemical reduction method (McIlvin and Altabet, 2005; Ryabenko et al., 2009) and  
141 University of California at Davis' Stable Isotope Facilities using the denitrifier method (Sigman et al.,  
142 2001). The isotope analysis was conducted using a Thermo Finnigan MAT 252 coupled with a  
143 GasBench II interface; isotope values are presented in per mil (‰) with respect to AIR for  $\delta^{15}\text{N}$  and



6

144 VSMO for  $\delta^{18}\text{O}$  with a precision of 0.3-0.4‰ and 0.5-0.6‰ for  $\delta^{15}\text{N}$ -nitrate and  $\delta^{18}\text{O}$ -nitrate,  
145 respectively.  
146  
147 Seawater samples for determining carbonate chemistry variables (pH on the total scale, TA, and DIC)  
148 were collected from the 5 sampling sites using a peristaltic pump and pressure filtering seawater  
149 through a 0.45- $\mu\text{m}$  filter. Samples for pH ( $\pm 0.005$ ) were filtered into 30-mL optical glass cells and  
150 analyzed within 1 hr of collection using spectrophotometric methods (Zhang and Byrne, 1996), an  
151 Ocean Optics USB2000 spectrometer, and thymol blue indicator dye. Samples for TA ( $\pm 1 \mu\text{mol kg}^{-1}$ )  
152 and DIC ( $\pm 2 \mu\text{mol kg}^{-1}$ ) were filtered into 300-ml borosilicate glass bottles, preserved by adding 100  
153  $\mu\text{L}$  saturated  $\text{HgCl}_2$  solution and pressure sealed with ground glass stoppers coated with Apiezon  
154 grease. TA samples were analyzed using spectrophotometric methods of (Yao and Byrne, 1998) with  
155 an Ocean Optics USB2000 spectrometer and bromocresol purple indicator dye. DIC samples were  
156 analyzed using a UIC carbon coulometer model CM5014 and CM5130 acidification module fitted with  
157 a sulfide scrubber, and methods of (Dickson et al., 2007). In-situ temperatures recorded from Solonist  
158 CTD Divers were reported and used to temperature-correct pH and perform CO2SYS calculations as  
159 described below.  
160  
161 Certified reference materials (CRM) for TA and DIC analyses were from the Marine Physical  
162 Laboratory of Scripps Institution of Oceanography (Dickson et al., 2007). Duplicate or triplicate  
163 analyses were performed on at least 10% of samples, yielding a mean precision of  $\sim 1 \mu\text{mol kg}^{-1}$  and  $\sim 2$   
164  $\mu\text{mol kg}^{-1}$  for TA and DIC analyses, respectively. The full seawater  $\text{CO}_2$  system was calculated with  
165 measured salinity, temperature, nutrients (phosphate and silicate), TA, DIC, and pH data using an  
166 Excel Workbook Macro translation of the original CO2SYS program (Pierrot et al., 2006). Given the  
167 enriched nutrient setting of the study site, TA values were nutrient corrected in CO2SYS (Dickson,  
168 1981). The aragonite saturation state and  $p\text{CO}_2$  are reported based on TA-pH pairs, with dissociation  
169 constants  $K_1$  and  $K_2$  from (Mehrbach et al., 1973) refit by (Dickson and Millero, 1987) and  $\text{KSO}_4$  from  
170 (Dickson, 1990). The TA and DIC values were normalized to salinity (by multiplying by a factor of  
171  $35/S$ , where  $S$  is the measured salinity value) to account for variations in TA and DIC driven by  
172 evaporation and/or precipitation (Friis et al., 2003) and are reported as  $n\text{TA}$  and  $n\text{DIC}$  as previously  
173 established in reef geochemical surveys (e.g., Suzuki and Kawahata, 2003; Yates et al., 2014;  
174 Muehllehner et al., 2016). However at the vent site the TA and DIC data was not normalized to salinity  
175 given the contribution of TA and DIC from SGD.  
176



### 177 3. Results

#### 178 3.1 Submarine Groundwater Endmember

179 The magnitude of change and absolute values in the carbonate chemistry, nutrients, and salinity were  
180 greatest at the primary vent site relative to the four sites along the reef. The salinity ranged from 10.64  
181 to 36.72 over the 6-d period (Fig. 2A), with the most dramatic decrease in salinity on March 22<sup>nd</sup> when  
182 salinity decreased from 32.45 to 12.47 within 4 hr. The reduction in salinity was sustained over a 32-hr  
183 period. A rapid change was also observed in the pH, DO, TA, DIC, and nutrient concentrations (Fig.  
184 2). For example, nitrate concentrations at the vent site ranged from 0.45 to over 70  $\mu\text{mol L}^{-1}$ , with an  
185 average nitrate concentration of 117 (SD 0.09)  $\mu\text{mol L}^{-1}$  measured directly from the discharging seep  
186 water. The  $\Omega_{\text{arag}}$  values decreased to less than 1 and  $p\text{CO}_2$  values increased to 2000  $\mu\text{atm}$  when salinity  
187 values dropped to less than 15 (Fig. 2D). No diurnal pattern was detected in the seawater carbonate  
188 chemistry at this site. Instead, these results are consistent with earlier work documenting lower pH,  
189 nutrient enriched freshwater endmember values tightly coupled to SGD ( Swarzenski et al., 2012;  
190 Glenn et al., 2013; Swarzenski et al., 2016).

191

#### 192 3.2 Reef Flat

193 In contrast to the vent site, the overall magnitude of carbonate chemistry variation at the other four  
194 sites along the reef flat was less, and the signal was coherent among these sites. This coherency is  
195 captured in the pH time series (Fig. 3B), where the pH data from the four sites were significantly  
196 ( $p < 0.05$ ) positively correlated with each other (with  $r \sim 0.5$ ). The lowest salinity value along the reef  
197 flat was 33.51, indicating minimal freshwater influence on reef flat salinity. As a result, the carbonate  
198 system parameters measured along the reef were non-linear with respect to salinity, instead a diurnal  
199 pattern dominated the signal (Fig. 3). Lowest pH values occurred around midnight (23:00); and highest  
200 pH values occurred in the afternoon (~14:00-15:00). This diurnal pattern was also apparent in the DIC  
201 data, with lowest values in the afternoon and increasing around midnight, with a cubic spline fit (Press  
202 et al., 1988) highlighting diurnal cycle from all four sites along the reef flat. Likewise, the diurnal  
203 signal was identifiable in the  $\Omega_{\text{arag}}$  and  $p\text{CO}_2$  time-series, with  $\Omega_{\text{arag}}$  values increasing and  $p\text{CO}_2$   
204 decreasing during the mid-day hours (Fig. 3). The diurnal signal in the  $n\text{TA}$  time-series was similar to  
205 the signal for  $n\text{DIC}$ . At the shallow (<5 m) sites, pH and DO covaried ( $r^2 = 0.43-0.87$ ;  $p < 0.001$ ). The  
206 range in pH and  $\Omega_{\text{arag}}$  was largest at the shallow sites; however, the average values were similar along  
207 the reef, 3.02 to 3.06 and 8.00 to 8.01, respectively, and were elevated relative to the average values  
208 recorded at the vent site, 7.85 (SD 0.17) and 2.28 (SD 0.81) for pH and  $\Omega_{\text{arag}}$ , respectively (Prouty et  
209 al., 2017b). No diurnal pattern was observed for the nutrient data; however, there was an offshore



210 gradient in nutrient concentrations with enriched nutrients at the shallow sites compared to the deeper  
211 sites. Nutrient concentrations ( $\text{Si}$ ,  $\text{PO}_4^{3-}$ , and  $\text{NO}_3^-$ ) from the two shallow sites were statistically greater  
212 than the two deeper sites according to pairwise multi-comparison one-way ANOVA with a *post hoc*  
213 Tukey HSD ( $p > 0.05$ ). For example average nitrate concentrations at the two shallow sites were 0.71  
214 (SD 0.35) and 0.41 (0.18 SD) compared to 0.17 (SD 0.10) and 0.19 (SD 0.11)  $\mu\text{mol L}^{-1}$ . Deficits and  
215 surpluses of  $n\text{TA}$  and  $n\text{DIC}$ , with respect to open ocean conditions, were calculated as  $\Delta n\text{TA}$  and  
216  $\Delta n\text{DIC}$  using values from Station HOT (Dore et al., 2009), located approximately 250 km offshore.  
217 The  $\Delta n\text{TA}$  values ranged from  $-332 \mu\text{mol kg}^{-1}$  to  $85 \mu\text{mol kg}^{-1}$  and  $-171 \mu\text{mol kg}^{-1}$  to  $141 \mu\text{mol kg}^{-1}$   
218  $\Delta n\text{DIC}$ . The standard error of difference ( $\text{SE}_{\text{dif}}$ ) was calculated for  $\Delta n\text{TA}$  and  $\Delta n\text{DIC}$  values to evaluate  
219 whether the deficits and surpluses of  $n\text{TA}$  and  $n\text{DIC}$  were significant. Histogram plots reveal statistical  
220 ( $p = 0.05$ ; critical  $t$  value of 1.68;  $\text{df} = 37$ ) deficits and surpluses as well as differences between the first  
221 and second half of the sampling period (Fig. 4). Results show a shift from a deficit in  $\Delta n\text{TA}$  to a  
222 surplus in  $\Delta n\text{TA}$  at all stations, as well as a shift from a deficit in  $\Delta n\text{DIC}$  to a surplus in  $\Delta n\text{DIC}$ ,  
223 suggesting a shift in the second sampling period from net  $\text{CaCO}_3$  production to net  $\text{CaCO}_3$  dissolution,  
224 and from net photosynthesis to net respiration. This change was most distinct at the two shallow sites.  
225 The  $n\text{TA}$  and  $n\text{DIC}$  values from the second sampling period were also enriched relative to a range of  
226 values reported from nearshore Oahu sites (Drupp et al., 2013).

227

#### 228 4. Discussion

229 The diurnal pattern observed at the four sampling sites along the reef flat is typical of a reef  
230 environment where biotic processes involving coral reef community metabolism (e.g.,  
231 respiration/photosynthesis and calcification/dissolution) dominate the carbonate chemistry system  
232 (e.g., Smith, 1973). The non-linear relationship between salinity and carbonate chemistry parameters  
233 further supports the notion that biotic processes are driving carbonate chemistry variability along the  
234 reef flat (Millero et al., 1998; Ianson et al., 2003). The lower amplitude  $n\text{TA}$  diurnal signal supports  
235 previous observations that the region was algal-dominated (Smith et al., 2005). In this case, the lower  
236 biomass of calcifying organisms leads to conditions that favor respiration-photosynthesis processes  
237 relative to calcification-dissolution (Jokiel et al., 2014). Elevated pH values during mid-day, coincident  
238 with elevated sea surface temperature (SST) and peak solar irradiance, are consistent with maximum  
239 photosynthetic activity. DIC decreased during the day due to photosynthesis, whereas at nighttime, pH  
240 decreased and DIC increased in response to respiration (Fig. 3). This pattern is in stark contrast to the  
241 primary vent site where no diurnal pattern was observed, and abiotic controls on the carbonate system  
242 dynamics explain the strong linear relation to salinity. Variability at the vent site is driven by SGD





243 rates, which are elevated during low tide when hydraulic gradients are the steepest (Dimova et al.,  
244 2012; Swarzenski et al., 2016).

245

246 To further understand the temporal variability in carbonate chemistry over the 6-d sampling period  
247 along the reef flat, diagrams of  $nTA$  versus  $nDIC$  were plotted according to Zeebe and Wolf-Gladrow,  
248 (2001), along with vectors indicating theoretical effects of organic and inorganic carbon metabolism on  
249 seawater chemistry (Kawahata et al., 1997; Suzuki and Kawahata, 2003) (Fig 5). Diagrams of  $nTA$ -  
250  $nDIC$  indicate the dominance of net community production (NCP) and net community calcification  
251 (NCC) during the first sampling period (16-19 March). The slope values of the  $nDIC$ - $nTA$  plots were  
252 used to calculate ratios of NCC:NEP (Table 1) using methods of Suzuki and Kawahata (2003). In the  
253 absence of reliable water mass residence time, ratios were used rather than metabolic rates. The  
254 NCC:NEP ratios for the first sampling period ranged from 0.50 to 0.87 indicate that both calcification  
255 and photosynthesis contributed to variability in carbonate system parameters with photosynthesis as  
256 the dominant processes in all cases. This pattern was observed at all four sites along the reef flat. In  
257 comparison, a shift occurred after the first sampling period. Elevated  $nDIC$  and  $nTA$  values during 21-  
258 24 March indicate a shift to primarily respiration and dissolution in the  $nTA$ - $nDIC$  diagrams (Fig. 5).  
259 At the shallow sites, S1 and S2 (Fig. 5A and B), the NCC:NCP ratios were 0.56 and 0.39 (Table 1),  
260 respectively, indicating primarily net respiration at these locations. On Heron Island for example, high  
261 organic production results in NCC:NCP ratios between 0.25 and 0.29 (McMahon et al., 2013; Albright  
262 et al., 2015). Dissolution and respiration contributed nearly equally with NCC:NCP ratios near 1.0 at  
263 sites S3 and S4 located further offshore. Rather than reflecting an artifact of the salinity normalization,  
264 given the non-linear relation of DIC and TA to salinity along the reef flat, this shift is interpreted as a  
265 reef community response. As shown in Figures 4 and 5, this change captures a shift from a reef  
266 community dominated by calcification to one dominated by respiration and dissolution.

267

268 The shift from net photosynthesis (P) to net respiration (R) as captured in the  $\Delta nDIC$  histogram plots  
269 (Fig. 4), suggests that the coral-algal association consumed more energy than it produced during the  
270 second sampling period. As a proxy for autotrophic capacity, the change in P:R ratio may reflect an  
271 increase in coral heterotrophic feeding relative to autotrophic feeding (Coles and Jokiel, 1977; Hughes  
272 and Grottoli, 2013). Typically, stored lipid reserves in the tissue are utilized when the stable symbiotic  
273 environment is disturbed (e.g., Szmant and Gassman, 1990; Ainsworth et al., 2008). Although short-  
274 lived, thermally-induced bleaching has been linked to depletion of coral lipid reserves (e.g., Hughes  
275 and Grottoli, 2013), excess nutrient loading can also shift the stability of the coral-algae symbiosis,



276 thereby reducing stored tissue reserves (Wooldridge, 2016). According to Glenn et al. (2013), up to 11  
277  $\text{m}^3 \text{d}^{-1}$  of dissolved inorganic nitrogen are discharged onto the West Maui reef as the result of receiving  
278 and treating over 15,000  $\text{m}^3 \text{d}^{-1}$  of sewage. Using a SGD flux rate of  $87 \text{ cm d}^{-1}$  at the primary seep site  
279 (Swarzenski et al., 2016), and SGD nitrate end-member concentration of  $117 \mu\text{mol L}^{-1}$  (Prouty et al.,  
280 2017b), the nitrate flux from the primary vent site is  $712 \text{ mol d}^{-1}$ , clearly demonstrating excess nutrient  
281 loading. As described above, an offshore gradient in nutrient concentrations was observed with  
282 enriched nutrients at the shallow sites compared to the deeper sites, consistent with a decrease in coral  
283  $\delta^{15}\text{N}$  values away from the vent (Prouty et al., 2017a). Coral tissue thickness was also negatively  
284 correlated to coral tissue  $\delta^{15}\text{N}$  values ( $r = -0.66$ ;  $p = 0.08$ ), with the latter serving as a proxy for  
285 nutrient loading in alga samples along the reef flat (Dailer et al., 2010). It is possible that a reduction in  
286 coral tissue reflects preferential heterotrophic feeding under high nutrient loading, with nutrient  
287 enrichment by sewage effluent increasing primary production and biomass in the water column (e.g.,  
288 Smith et al., 1981; Pastorok and Bilyard, 1985). While assessing the impacts of nutrient loading on  
289 coral physiology may be long term and subtle in some cases, results from our study highlight the  
290 potential short-term impacts of nitrification on the short term.

291  
292 Identifying the exact mechanism(s) responsible for driving this shift is difficult given the complexity of  
293 the reef system. Possible explanations include warmer SSTs, suspension of organic matter, as well as  
294 secondary effects of nitrification from contaminated SGD (D'Angelo and Wiedenmann, 2014).  
295 Given that microbial communities rapidly take up inorganic nutrients (Furnas et al., 2005), there could  
296 be increased respiration as a result of increased microbial remineralization of organic matter in the  
297 nutrient-loaded environment. In other words, enhanced SGD- driven nutrient fluxes during the second  
298 sampling period could have increased microbial growth and remineralization, shifting the reef  
299 community metabolism, as captured in a shift in the carbonate chemistry system. In addition to  
300 community metabolism, local oceanographic effects such as the wind and wave regime can also drive  
301 carbonate chemistry by altering air-sea exchange and water mass residence times. During the first  
302 sampling period, the wave height increased from 0.4 m to 1.6 m over the first 2 d and mean current  
303 speeds were  $1.6 \text{ cm s}^{-1}$  (Fig. S1). In comparison, during the second sampling period, wave height  
304 declined to less than 0.4 m and mean current speeds were  $1.0 \text{ cm s}^{-1}$ . Together, the reduced wave  
305 height and reduced wind speeds favor slower release of  $\text{CO}_2$  generated by calcification and respiration  
306 processes from the water column (Massaro et al., 2012), resulting in higher  $p\text{CO}_2$  and lower pH.

307  
308 Despite being situated in an oligotrophic region with naturally occurring, low nutrient concentrations,



309 anthropogenic nutrient loading to coastal waters via sustained SGD is driving nearshore eutrophication  
310 ( Dailer et al., 2010; Dailer et al., 2012; Bishop et al., 2015; Amato et al., 2016; Fackrell et al., 2016),  
311 with algal  $\delta^{15}\text{N}$  signatures at Kahekili Beach Park indicative of wastewater effluent (Dailer et al.,  
312 2010; Dailer et al., 2012). In response, there has been a shift in benthic cover from abundant corals to  
313 turf- or macro-algae over the last two decades. Areas of discrete coral cover loss up to 100% along the  
314 shallow coral reef at Kahekili have been observed for decades ( Wiltse, 1996; Ross et al., 2012), with a  
315 history of macro-algal blooms (Smith et al., 2005). More recently, Prouty et al. (2017a) found  
316 accelerated nutrient driven-bioerosion from coral cores collected along the Kahekili reef flat in  
317 response to land-based sources of nutrients. This is consistent with earlier work showing nitrification-  
318 mediated increase in plankton loads can trigger increases in filter feeders and bioeroders that endanger  
319 reef structure integrity (e.g., Fabricius et al., 2012). Eutrophication from nutrient enriched SGD may  
320 contribute to an already compromised carbonate system (i.e., reduced pH and  $\Omega_{\text{arag}}$ ) by increasing net  
321 respiration and remineralization of excess organic matter, and increasing bioerosion. Therefore,  
322 secondary effects of nutrient-driven increase in phytoplankton biomass and decomposing organic  
323 matter are also important considerations for coral reef management (D'Angelo and Wiedenmann,  
324 2014).

325

326 As discussed above, SGD rates are elevated during low tide when the relative pressure head between  
327 terrestrial groundwater and the oceanic water column is greatest (Dimova et al., 2012; Swarzenski et  
328 al., 2016). Relative SGD is greater in the shallows close to shore where the tidal height is larger  
329 relative to the depth of the water column. Higher islands, therefore, have the potential for not only  
330 greater orographic rainfall and thus submarine groundwater recharge, but also greater potential  
331 pressure head and thus enhanced SGD- driven nutrient fluxes. There is also greater potential for  
332 enriched nutrient sources and reduced water quality with fast-growing population and development  
333 (Amato et al., 2016; Fackrell et al., 2016). Thus, SGD represents a key vector of nutrient loading in  
334 tropical, oligotrophic regions (e.g., Paytan et al., 2006). At the same time, closer to shore, current  
335 speeds are generally slower resulting in longer water mass residence times (Storlazzi et al., 2006);  
336 longer residence times would also be expected closer to the seabed, compared with upper water  
337 column flows (Storlazzi and Jaffe, 2008). Together, these suggest that the resulting exposure (=   
338 intensity x residence time) of coral reefs to nutrient-laden, low pH submarine groundwater is greater  
339 for coral reefs closer to shore off high islands than along barrier reefs or on atolls. This heightened  
340 vulnerability therefore needs to be taken into account when evaluating vulnerability of nearshore  
341 fringing reefs to changes in carbonate chemistry system given evidence of nutrient driven-bioerosion



342 from land-based sources of pollution.

343

344

### 345 **5. Conclusion**

346 Field based measurements of carbonate chemistry variability were made along a shallow coral reef off  
347 Kahekili, west Maui, and captured differences in the relative importance of inorganic and organic  
348 carbon production over a 6-d period in March 2016. Submarine groundwater discharge fluxes  
349 controlled the carbonate chemistry adjacent to the primary vent site, with nutrient-laden freshwater  
350 decreasing the pH levels and favoring undersaturated  $\Omega_{\text{arag}}$  conditions. In contrast, reef community  
351 metabolism dominated the carbonate chemistry diurnal signal at sites along the reef flat. Superimposed  
352 on the diurnal signal was a transition during the second sampling period, yielding a surplus of  $n\text{TA}$  and  
353  $n\text{DIC}$  compared to ocean endmember measurements indicating a shift from net photosynthesis and  
354 calcification to net respiration and carbonate dissolution. This shift could be interpreted as a direct  
355 response to increased nutrient loading, and subsequent enhancement of organic matter  
356 remineralization. Predictions of reef response to elevated  $p\text{CO}_2$  levels assume reef water tracks open-  
357 ocean pH, however local effects are equally important (e.g., Cyronak et al., 2013), particularly along  
358 densely-inhabited shorelines with known input from land-based sources of pollution. Building on  
359 previous work documenting the input of nutrient laden, low-pH freshwater to the reefs off Kahekili,  
360 results presented here offer a first glimpse into how anthropogenic-driven eutrophication might add an  
361 additional stressor to thresholds tipping the balance between net carbonate accretion and net carbonate  
362 dissolution, thus altering carbonate system dynamics.

363

### 364 **Author contribution**

365 NGP and KKY designed the experiments and NGP, KKY, NS and CG carried them out. NGP and  
366 KKY completed the chemical measurements and OC compiled the oceanographic data. NGP prepared  
367 the manuscript with contributions from all co-authors.

368

369 The authors declare that they have no conflict of interest.

370

### 371 **Acknowledgements**

372 This research was carried out as part of the US Geological Survey's Coral Reefs Project in an effort to  
373 better understand the effects of geologic and oceanographic processes on coral reef systems in the  
374 USA and its trust territories, and was supported by the USGS Coastal and Marine Geology Program.  
375 The authors gratefully acknowledge the vital partnership and expert logistics support provided by the  
376 State of Hawaii Division of Aquatic Resources. We thank T. DeCarlo (UWA), H. Barkley (NOAA) for



377 reviews, and A. Cohen (WHOI) for helpful discussions, K.R. Pietro and K. Hoering (WHOI), C.  
378 Moore (USGS), and G. Paradis (UCSB) analytical assistance, M. Dailer (U. Hawaii) for field  
379 assistance. The use of trade names is for descriptive purposes only and does not imply endorsement by  
380 the U.S. Government.

381

### 382 **Figure Captions**

383 **Figure 1.** Location map of the island of Maui, Hawaii, USA, and the study area along west Maui.  
384 Bathymetric map (5-m contours) of study area showing seawater sampling locations (blue closed  
385 circle) along Kahekili Beach Park, and the primary seep site (blue open circle) superimposed on  
386 distribution of percent coral cover versus sand.

387

388 **Figure 2** Results of time-series of seawater chemistry variables over a 6-d period collected from  
389 bottom water near the seep site on the nearshore reef every 4 hr. (A) Salinity, (B) dissolved nutrient  
390 (nitrate+nitrite, phosphate, and silicate) concentrations ( $\mu\text{mol L}^{-1}$ ), and nitrate stable nitrogen isotopes  
391 ( $\delta^{15}\text{N}$ -nitrate; ‰), (C) total alkalinity (TA) and dissolved inorganic carbon (DIC) ( $\mu\text{mol kg}^{-1}$ ), (D)  
392 calculated carbonate parameters for aragonite saturation state ( $\Omega_{\text{arag}}$ ), and  $p\text{CO}_2$  ( $\mu\text{atm}$ ; inverted) based  
393 on TA-pH pairwise and measured salinity, temperature, nutrients (phosphate and silicate) data, (E)  
394 dissolved oxygen (DO;  $\text{mg L}^{-1}$ ), and (F) temperature corrected pH (total scale). End-of-century  
395 projections according to IPCC-AR5 RCP8.5 “business as usual” scenario for pH (reduction by 0.4  
396 units),  $\Omega_{\text{arag}}$  (2.0; blue dashed), and  $p\text{CO}_2$  (750  $\mu\text{atm}$ ; red dashed).

397

398 **Figure 3** Carbonate chemistry parameters and sea surface temperature (SST) composite from S1, S2,  
399 S3 and S3 along the shallow reef flat of Kahekili, Maui and cubic spline fits highlighting diurnal cycle  
400 for the first (16-19 March 2016; solid line) and second (21-24 March 2016; dashed line) sampling  
401 period for (A) Temperature, (B) pH, (C)  $n\text{DIC}$  and (D)  $n\text{TA}$  ( $\mu\text{mol kg}^{-1}$ ), (E)  $\Omega_{\text{arag}}$  and (F)  $p\text{CO}_2$   
402 ( $\mu\text{atm}$ ).

403

404 **Figure 4** Histogram  $\Delta n\text{TA}$  and  $\Delta n\text{DIC}$  capturing deficits and surpluses of  $n\text{TA}$  and  $n\text{DIC}$  with respect  
405 to open ocean conditions. Overall a transition from net  $\text{CaCO}_3$  production to net  $\text{CaCO}_3$  dissolution  
406 and net photosynthesis to net respiration occurred between the first (16-19 March 2016; blue) and  
407 second (21-24 March 2016; red) sampling period for the shallow sampling sites (A)-(B) S1 and (C)-  
408 (D) S2, and the two deeper sites (E)-(F) S3, and (G-H) S4. Statistical ( $p=0.05$ ) deficit and surplus  
409 values ( $\pm$ ) for  $\Delta n\text{TA}$  and  $\Delta n\text{TA}$  shown in parentheses.



410

411 **Figure 5** Seawater carbonate chemistry system along the reef flat off Kahekili as a function of  $nDIC$   
412 and  $nTA$  for the shallow sampling sites (A). S1 and (B) S2, and two deeper sites (C) S3, and (D) S4 for  
413 the first (blue) and second (red) sampling periods and their respective slopes (solid lines) of  $nDIC$  and  
414  $nTA$  (Table 1) and theoretical slope (dashed lines) given the predicted effects of photosynthesis,  
415 respiration, calcification, and dissolution as shown in (E) and the respective change in net community  
416 calcification (NCC) and net community production (NCP).

417

#### 418 References

- 419 Ainsworth, T. D., Hoegh-Guldberg, O., Heron, S. F., Skirving, W. J., and Leggat, W.: Early cellular  
420 changes are indicators of pre-bleaching thermal stress in the coral host, *J Exp Mar Biol Ecol*,  
421 364, 63-71, [10.1016/j.jembe.2008.06.032](https://doi.org/10.1016/j.jembe.2008.06.032), 2008.
- 422 Albright, R., Benthuyssen, J., Cantin, N., Caldeira, K., and Anthony, K.: Coral reef metabolism and  
423 carbon chemistry dynamics of a coral reef flat, *Geophys Res Lett*, 42, 3980-3988,  
424 [10.1002/2015GL063488](https://doi.org/10.1002/2015GL063488), 2015.
- 425 Amato, D. W., Bishop, J. M., Glenn, C. R., Dulai, H., and Smith, C. M.: Impact of submarine  
426 groundwater discharge on marine water quality and reef biota of Maui, *PloS one*, 11,  
427 [e0165825](https://doi.org/10.1371/journal.pone.0165825), [10.1371/journal.pone.0165825](https://doi.org/10.1371/journal.pone.0165825) 2016.
- 428 Anderson, D. M., Glibert, P. M., and Burkholder, J. M.: Harmful algal blooms and eutrophication:  
429 nutrient sources, composition and consequences., *Estuaries*, 25, 562-584.,  
430 [10.1007/BF02804901](https://doi.org/10.1007/BF02804901), 2002.
- 431 Andersson, A. J., and Gledhill, D.: Ocean acidification and coral reefs: effects on breakdown,  
432 dissolution, and net ecosystem calcification, *Annual Review of Marine Science*, 5, 321-348,  
433 2013.
- 434 Andrefouet, S., Mumby, P. J., McField, M., Hu, C., and Muller-Karger, F. E.: Revisiting coral reef  
435 connectivity, *Coral Reefs*, 21, 43-48, [10.1007/s00338-001-0199-0](https://doi.org/10.1007/s00338-001-0199-0), 2002.
- 436 Bernstein, W. N., Huguen, K. A., Langdon, C., McCorkle, D. C., and Lentz, S. J.: Environmental  
437 controls on daytime net community calcification on a Red Sea reef flat, *Coral Reefs*, 35, 697-  
438 711, 2016.
- 439 Bishop, J. M., Glenn, C. R., Amato, D. W., and Dulai, H.: Effect of land use and groundwater flow  
440 path on submarine groundwater discharge nutrient flux, *Journal of Hydrology: Regional  
441 Studies*, [10.1016/j.ejrh.2015.10.008](https://doi.org/10.1016/j.ejrh.2015.10.008), 2015.
- 442 Cochran, S. A., Gibbs, A. E., and D.J., W.: Benthic habitat map of the U.S. Coral Reef Task Force  
443 Watershed Partnership Initiative Kā'anapali priority study area and the State of Hawai'i  
444 Kahekili Herbivore Fisheries Management Area, west-central Maui, Hawai'i, p. 42 p., U.S.  
445 Geological Survey Open-File Report 2014-1129, 2014.
- 446 Coles, S. L., and Jokiel, P. L.: Effects of temperature on photosynthesis and respiration in hermatypic  
447 corals, *Mar Biol*, 43, 209-216, [10.1007/BF00402313](https://doi.org/10.1007/BF00402313), 1977.
- 448 Cyronak, T., Santos, I. R., and Eyre, B. D.: Permeable coral reef sediment dissolution driven by  
449 elevated  $pCO_2$  and pore water advection, *Geophys Res Lett*, 40, 4876-4881,  
450 [10.1002/grl.50948](https://doi.org/10.1002/grl.50948), 2013.
- 451 Dailer, M. L., Knox, R. S., Smith, J. E., Napier, M., and Smith, C. M.: Using  $\delta^{15}N$  values in algal  
452 tissue to map locations and potential sources of anthropogenic nutrient inputs on the island of  
453 Maui, Hawai'i, USA, *Mar Pollut Bull*, 60, 655-671, [10.1016/j.marpolbul.2009.12.021](https://doi.org/10.1016/j.marpolbul.2009.12.021), 2010.



- 454 Dailer, M. L., Ramey, H. L., Saephan, S., and Smith, C. M.: Algal  $\delta^{15}\text{N}$  values detect a wastewater  
455 effluent plume in nearshore and offshore surface waters and three-dimensionally model the  
456 plume across a coral reef on Maui, Hawai'i, USA, *Mar Pollut Bull*, 64, 207-213,  
457 10.1016/j.marpolbul.2011.12.004, 2012.
- 458 DeCarlo, T. M., Cohen, A. L., Wong, G. T. F., Shiah, F. K., Lentz, S. J., Davis, K. A., Shamberger, K.  
459 E. F., and Lohmann, P.: Community production modulates coral reef pH and the sensitivity of  
460 ecosystem calcification to ocean acidification, *Journal of Geophysical Research: Oceans*, 122,  
461 2017.
- 462 Dickson, A. G.: An exact definition of total alkalinity and a procedure for the estimation of alkalinity  
463 and total inorganic carbon from titration data, *Deep-Sea Res*, 28A, 609-623, 1981.
- 464 Dickson, A. G.: Thermodynamics of the dissociation of boric acid in synthetic seawater from 273.15 to  
465 318.15 K, *Deep Sea Research Part A. Oceanographic Research Papers*, 37, 755-766,  
466 10.1016/0198-0149(90)90004-F, 1990.
- 467 Dickson, A. G., and Millero, F. J.: A comparison of the equilibrium constants for the dissociation of  
468 carbonic acid in seawater media, *Deep Sea Research Part A. Oceanographic Research Papers*,  
469 34, 1733-1743, 10.1016/0198-0149(87)90021-5, 1987.
- 470 Dickson, A. G., Sabine, C. L., and Christian, J. R.: Guide to best practices for ocean CO<sub>2</sub>  
471 measurements, PICES Special Publication, 3, 176, 2007.
- 472 Dimova, N. T., Swarzenski, P. W., Dulaiova, H., and Glenn, C. R.: Utilizing multichannel electrical  
473 resistivity methods to examine the dynamics of the fresh water-seawater interface in two  
474 Hawaiian groundwater systems, *Journal of Geophysical Research: Oceans*, 117,  
475 10.1029/2011jc007509, 2012.
- 476 Dore, J. E., Lukas, R., Sadler, D. W., Church, M. J., and Karl, D. M.: Physical and biogeochemical  
477 modulation of ocean acidification in the central North Pacific, *Proceedings of the National  
478 Academy of Sciences*, 106, 12235-12240, 2009.
- 479 Drupp, P. S., De Carlo, E. H., Mackenzie, F. T., Sabine, C. L., Feely, R. A., and Shamberger, K. E.:  
480 Comparison of CO<sub>2</sub> dynamics and air-sea gas exchange in differing tropical reef  
481 environments, *Aquat Geochem*, 19, 371-397, 2013.
- 482 Fabricius, K. E.: Effects of terrestrial runoff on the ecology of corals and coral reefs: review and  
483 synthesis, *Mar Poll Bull*, 50, 125-146, 10.1016/j.marpolbul.2004.11.028, 2005.
- 484 Fackrell, J. K., Glenn, C. R., Popp, B. N., Whittier, R. B., and Dulai, H.: Wastewater injection, aquifer  
485 biogeochemical reactions, and resultant groundwater N fluxes to coastal waters: Kā'anapali,  
486 Maui, Hawai'i, *Mar Pollut Bull*, 110, 281-292, 10.1016/j.marpolbul.2016.06.050, 2016.
- 487 Ferrario, F., Beck, M. W., Storlazzi, C. D., Micheli, F., Shepard, C. C., and Airoidi, L.: The  
488 effectiveness of coral reefs for coastal hazard risk reduction and adaptation, *Nature  
489 Communications*, 5, 10.1038/ncomms4794, 2014.
- 490 Friis, K., Körtzinger, A., and Wallace, D. W. R.: The salinity normalization of marine inorganic carbon  
491 chemistry data, *Geophys Res Lett*, 30, 2003.
- 492 Furnas, M., Mitchell, A., Skuza, M., and Brodie, J.: In the other 90%: phytoplankton responses to  
493 enhanced nutrient availability in the Great Barrier Reef Lagoon, *Mar Pollut Bull*, 51, 253-265,  
494 10.1016/j.marpolbul.2004.11.010, 2005.
- 495 Glenn, C. R., Whittier, R. B., Dailer, M. L., Dulaiova, H., El-Kadi, A. I., Fackrell, J., Kelly, J. L.,  
496 Waters, C. A., and Sevadjan, L.: Lahaina Groundwater Tracer Study – Lahaina, Maui, Hawaii,  
497 Final Report, p. 502 p., State of Hawaii Department of Health, the U.S. Environmental  
498 Protection Agency, and the U.S. Army Engineer Research and Development Center, 2013.
- 499 Howarth, R., Anderson, D., Cloern, J., Elfring, C., Hopkinson, C., Lapointe, B., Malone, T., Marcus,  
500 N., McGlathery, K., Sharpley, A., and Walker, D.: Nutrient pollution of coastal rivers, bays,  
501 and seas., *Issues Ecol*, 1 – 15, 2000.



- 502 Hughes, A. D., and Grottole, A. G.: Heterotrophic compensation: A possible mechanism for resilience  
503 of coral reefs to global warming or a sign of prolonged stress?, *PLOS ONE*, 8, e81172,  
504 10.1371/journal.pone.0081172, 2013.
- 505 Hughes, T. P., Baird, A. H., Bellwood, D. R., Card, M., Connolly, S. R., Folke, C., Grosberg, R.,  
506 Hoegh-Guldberg, O., Jackson, J. B. C., Kleypas, J., Lough, J. M., Marshall, P., Nystrom, M.,  
507 Palumbi, S. R., Pandolfi, J. M., Rosen, B., and Roughgarden, J.: Climate change, human  
508 impacts, and the resilience of coral reefs, *Science*, 301, 929-933, 10.1126/science.1085046,  
509 2003.
- 510 Hughes, T. P., Rodrigues, M. J., Bellwood, D. R., Ceccarelli, D., Hoegh-Guldberg, O., McCook, L.,  
511 Moltschanowskyj, N., Pratchett, M. S., Steneck, R. S., and Willis, B.: Phase shifts, serbivory,  
512 and the resilience of coral reefs to climate change, *Curr Biol*, 17, 360-365,  
513 10.1016/j.cub.2006.12.049, 2007.
- 514 Ianson, D., Allen, S. E., Harris, S. L., Orians, K. J., Varela, D. E., and Wong, C. S.: The inorganic  
515 carbon system in the coastal upwelling region west of Vancouver Island, Canada, *Deep Sea*  
516 *Research Part I: Oceanographic Research Papers*, 50, 1023-1042, 10.1016/S0967-  
517 0637(03)00114-6, 2003.
- 518 Jokieli, P. L., Jury, C. P., and Ku'ulei, S. R.: Coral-algae metabolism and diurnal changes in the CO<sub>2</sub>-  
519 carbonate system of bulk sea water, *PeerJ*, 2, e378, 2014.
- 520 Kawahata, H., Suzuki, A., and Goto, K.: Coral reef ecosystems as a source of atmospheric CO<sub>2</sub>:  
521 evidence from pCO<sub>2</sub> measurements of surface waters, *Coral Reefs*, 16, 261-266,  
522 10.1007/s003380050082, 1997.
- 523 Knowlton, N., and Jackson, J. B. C.: Shifting baselines, local impacts, and global change on coral  
524 reefs, *PLoS Biol*, 6, e54, 2008.
- 525 Lantz, C. A., Atkinson, M. J., Winn, C. W., and Kahng, S. E.: Dissolved inorganic carbon and total  
526 alkalinity of a Hawaiian fringing reef: chemical techniques for monitoring the effects of ocean  
527 acidification on coral reefs, *Coral Reefs*, 33, 105-115, 2014.
- 528 Lapointe, B. E., Barile, P. J., Littler, M. M., and Littler, D. S.: Macroalgal blooms on southeast Florida  
529 coral reefs. II. Cross-shelf  $\delta^{15}\text{N}$  values provide evidence of widespread sewage enrichment.,  
530 *Harmful Algae*, 4, 1106-1122., 10.1016/j.hal.2005.06.004, 2005.
- 531 Massaro, R. F. S., De Carlo, E. H., Drupp, P. S., Mackenzie, F. T., Jones, S. M., Shamberger, K. E.,  
532 Sabine, C. L., and Feely, R. A.: Multiple factors driving variability of CO<sub>2</sub> exchange between  
533 the ocean and atmosphere in a tropical coral reef environment, *Aquat Geochem*, 18, 357-386,  
534 2012.
- 535 McIlvin, M. R., and Altabet, M. A.: Chemical conversion of nitrate and nitrite to nitrous oxide for  
536 nitrogen and oxygen isotopic analysis in freshwater and seawater, *Anal Chem*, 77, 5589-5595,  
537 10.1021/ac050528s, 2005.
- 538 McMahon, A., Santos, I. R., Cyronak, T., and Eyre, B. D.: Hysteresis between coral reef calcification  
539 and the seawater aragonite saturation state, *Geophys Res Lett*, 40, 4675-4679,  
540 10.1002/grl.50802, 2013.
- 541 Mehrbach, C., Culbertson, C. H., Hawley, J. E., and Pytkowicz, R. M.: Measurement of the apparent  
542 dissociation constants of carbonic acid in seawater at atmospheric pressure, *Limnol Oceanogr*,  
543 18, 897-907, 10.4319/lo.1973.18.6.0897, 1973.
- 544 Millero, F. J., Lee, K., and Roche, M.: Distribution of alkalinity in the surface waters of the major  
545 oceans, *Mar Chem*, 60, 111-130, 10.1016/S0304-4203(97)00084-4, 1998.
- 546 Muehllehner, N., Langdon, C., Venti, A., and Kadko, D.: Dynamics of carbonate chemistry,  
547 production, and calcification of the Florida Reef Tract (2009–2010): Evidence for seasonal  
548 dissolution, *Global Biogeochem Cycles*, 30, 661-688, 10.1002/2015GB005327, 2016.
- 549 Pastorok, R. A., and Bilyard, G. R.: Effects of sewage pollution on coral-reef communities, *Mar Ecol*  
550 *Prog Ser*, 175-189, 1985.





- 551 Paytan, A., Shellenbarger, G. G., Street, J. H., Gonneea, M. E., Davis, K., Young, M. B., and Moore,  
552 W. S.: Submarine groundwater discharge: An important source of new inorganic nitrogen to  
553 coral reef ecosystems, *Limnol Oceanogr*, 51, 343-348, 10.4319/lo.2006.51.1.0343, 2006.
- 554 Pierrot, D., Lewis, E., and Wallace, D. W. R.: MS Excel program developed for CO<sub>2</sub> system  
555 calculations, 2006.
- 556 Press, W. H., Flannery, B. P., Teukolsky, S. A., and Vetterling, W. T.: *Numerical Recipes in C*,  
557 Cambridge University Press, New York, 1988.
- 558 Prouty, N. G., Cohen, A., Yates, K. K., Storlazzi, C. D., Swarzenski, P. W., and White, D.:  
559 Vulnerability of Coral Reefs to Bioerosion From Land-Based Sources of Pollution, *Journal of*  
560 *Geophysical Research: Oceans*, 122, 9319-9331, 10.1002/2017JC013264, 2017a.
- 561 Prouty, N.G., Yates, K.K., Smiley, N.A., and Gallagher, C. Coral growth parameters and seawater  
562 chemistry, Kahekili, west Maui: U.S. Geological Survey data release, 10.5066/F7X34VPV,  
563 2017b.
- 564 Rodgers, K. u. S., Jokiel, P. L., Brown, E. K., Hau, S., and Sparks, R.: Over a decade of change in  
565 spatial and temporal dynamics of Hawaiian coral reef communities 1, *Pac Sci*, 69, 1-13,  
566 10.2984/69.1.1, 2015.
- 567 Ross, M., White, D., Aiwahi, M., Walton, M., Sudek, M., Lager, D., and Jokiel, P.: Characterization of  
568 “dead zones” and population demography of *Porites compressa* along a gradient of  
569 anthropogenic nutrient input at Kahekili Beach Park, Maui, State of Hawaii, Department of  
570 Land and Natural Resources, Division of Aquatic Resources, Honolulu, Hawaii 96813, 2012.
- 571 Ryabenko, E., Altabet, M. A., and Wallace, D. W. R.: Effect of chloride on the chemical conversion of  
572 nitrate to nitrous oxide for  $\delta^{15}\text{N}$  analysis, *Limnol Oceanogr*, Methods 7, 545-552,  
573 10.4319/lom.2009.7.545, 2009.
- 574 Shamberger, K. E. F., Feely, R. A., Sabine, C. L., Atkinson, M. J., DeCarlo, E. H., Mackenzie, F. T.,  
575 Drupp, P. S., and Butterfield, D. A.: Calcification and organic production on a Hawaiian coral  
576 reef, *Mar Chem*, 127, 64-75, 2011.
- 577 Shaw, E. C., McNeil, B. I., and Tilbrook, B.: Impacts of ocean acidification in naturally variable coral  
578 reef flat ecosystems, *Journal of Geophysical Research: Oceans*, 117, 2012.
- 579 Sigman, D. M., Casciotti, K. L., Andreani, M., Barford, C., Galanter, M., and Bohlke, J. K.: A  
580 bacterial method for the nitrogen isotopic analysis of nitrate in seawater and freshwater, *Anal*  
581 *Chem*, 73, 4145-4415, 10.1021/ac010088e, 2001.
- 582 Silverman, J., Lazar, B., and Erez, J.: Community metabolism of a coral reef exposed to naturally  
583 varying dissolved inorganic nutrient loads, *Biogeochemistry*, 84, 67-82, 2007.
- 584 Silverman, J., Lazar, B., Cao, L., Caldeira, K., and Erez, J.: Coral reefs may start dissolving when  
585 atmospheric CO<sub>2</sub> doubles, *Geophys Res Lett*, 36, 2009.
- 586 Smith, J. E., Runcie, J. W., and Smith, C. M.: Characterization of a large-scale ephemeral bloom of the  
587 green alga *Cladophora sericea* on the coral reefs of West Maui, Hawaii, *Mar Ecol Prog Ser*,  
588 302, 77-91, 2005.
- 589 Smith, S. V.: Carbon dioxide dynamics: a record of organic carbon production, respiration, and  
590 calcification in the Eniwetok reef flat community, *Limnol. Oceanogr*, 18, 106-120, 1973.
- 591 Smith, S. V., Kimmerer, W. J., Laws, E. A., Brock, R. E., and Walsh, T. W.: Kaneohe Bay sewage  
592 diversion experiment: perspectives on ecosystem responses to nutritional perturbation, *Pac*  
593 *Sci*, 35, 279-395, 1981.
- 594 Sparks, R. T., Stone, K., White, D. J., Ross, M., and Williams, I. D.: Maui and Lanai Monitoring  
595 Report, Hawaii Department of Land and Natural Resources, Division of Aquatic Resources,  
596 Maui, 130 Mahalani Street, Wailuku HI. 96790, 2016.
- 597 Storlazzi, C. D., McManus, M. A., Logan, J. B., and McLaughlin, B. E.: Cross-shore velocity shear,  
598 eddies and heterogeneity in water column properties over fringing coral reefs: West Maui,  
599 Hawaii, *Cont Shelf Res*, 26, 401-421, 2006.



- 600 Storlazzi, C. D., and Jaffe, B. E.: The relative contribution of processes driving variability in flow,  
601 shear, and turbidity over a fringing coral reef: West Maui, Hawaii, *Estuarine, Coastal and*  
602 *Shelf Science*, 77, 549-564, 10.1016/j.ecss.2007.10.012, 2008.
- 603 Suzuki, A., and Kawahata, H.: Carbon budget of coral reef systems: an overview of observations in  
604 fringing reefs, barrier reefs and atolls in the Indo-Pacific regions, *Tellus B*, 55, 428-444,  
605 10.1034/j.1600-0889.2003.01442.x, 2003.
- 606 Swarzenski, P., Dulai, H., Kroeger, K., Smith, C., Dimova, N., Storlazzi, C., Prouty, N., Gingerich, S.,  
607 and Glenn, C.: Observations of nearshore groundwater discharge: Kahekili Beach Park  
608 submarine springs, Maui, Hawaii, *Journal of Hydrology: Regional Studies*,  
609 10.1016/j.ejrh.2015.12.056, 2016.
- 610 Swarzenski, P. W., Storlazzi, C. D., Presto, M. K., Gibbs, A. E., Smith, C. G., Dimova, N. T., Dailer,  
611 M. L., and Logan, J. B.: Nearshore morphology, benthic structure, hydrodynamics, and coastal  
612 groundwater discharge near Kahekili Beach Park, Maui, Hawaii., p. 34 p., U.S. Geological  
613 Survey Open-File Report 2012–1166. 2012.
- 614 Swarzenski, P. W., Dulai, H., Dailer, M. L., Glenn, C. R., Smith, C. G., and Storlazzi, C. D.: A  
615 geochemical and geophysical assessment of coastal groundwater discharge at select sites in  
616 Maui and O’ahu, Hawai’i, in: *Groundwater in the Coastal Zones of Asia-Pacific*, edited by:  
617 Wetzelhuetter, C., Coastal Research Library, Springer Netherlands, 27-46, 2013.
- 618 Szmant, A., and Gassman, N. J.: The effects of prolonged “bleaching” on the tissue biomass and  
619 reproduction of the reef coral *Montastrea annularis*, *Coral Reefs*, 8, 217-224, 1990.
- 620 Wiltse, W.: *Algal Blooms: Progress Report on Scientific Research*. West Maui Watershed  
621 Management Project, 1996.
- 622 Wooldridge, S. A.: Excess seawater nutrients, enlarged algal symbiont densities and bleaching  
623 sensitive reef locations: 1. Identifying thresholds of concern for the Great Barrier Reef,  
624 Australia, *Mar Pollut Bull*, 10.1016/j.marpolbul.2016.04.054, 2016.
- 625 Yao, W., and Byrne, R. H.: Simplified seawater alkalinity analysis: use of linear array spectrometers,  
626 *Deep Sea Research Part I: Oceanographic Research Papers*, 45, 1383-1392, 1998.
- 627 Yates, K. K., Zawada, D. G., Smiley, N. A., and Tiling-Range, G.: Divergence of seafloor elevation  
628 and sea level rise in coral reef ecosystems, *Biogeosciences*, 14, 1739-1772, 10.5194/bg-14-  
629 1739-2017, 2017.
- 630 Zeebe, R. E., and Wolf-Gladrow, D. A.: *CO<sub>2</sub> in seawater: equilibrium, kinetics, isotopes*, Gulf  
631 Professional Publishing, 2001.
- 632 Zhang, H., and Byrne, R. H.: Spectrophotometric pH measurements of surface seawater at in-situ  
633 conditions: absorbance and protonation behavior of thymol blue, *Mar Chem*, 52, 17-25,  
634 10.1016/0304-4203(95)00076-3, 1996.
- 635  
636



637

Site	<i>n</i> TA- <i>n</i> DIC Slope	NCC:NCP	$r^2$
<i>16-19 March 2016</i>			
S1	0.88	0.78	0.94
S2	0.67	0.50	0.75
S3	0.93	0.88	0.89
S4	0.93	0.87	0.92
<i>21-24 March 2016</i>			
S1	0.72	0.56	0.78
S2	0.56	0.39	0.77
S3	0.99	0.98	0.95
S4	1.04	1.08	0.94

638

639 **Table 1**640 Slope of salinity normalized total alkalinity (*n*TA): salinity normalized dissolved inorganic carbon

641 (DIC), net community calcification: net community production ratio (NCC:NCP=2ΔDIC/ΔTA-1)

642 (Suzuki and Kawahata, 2003) and correlation coefficients ( $r^2$ ).

643



Figure 1

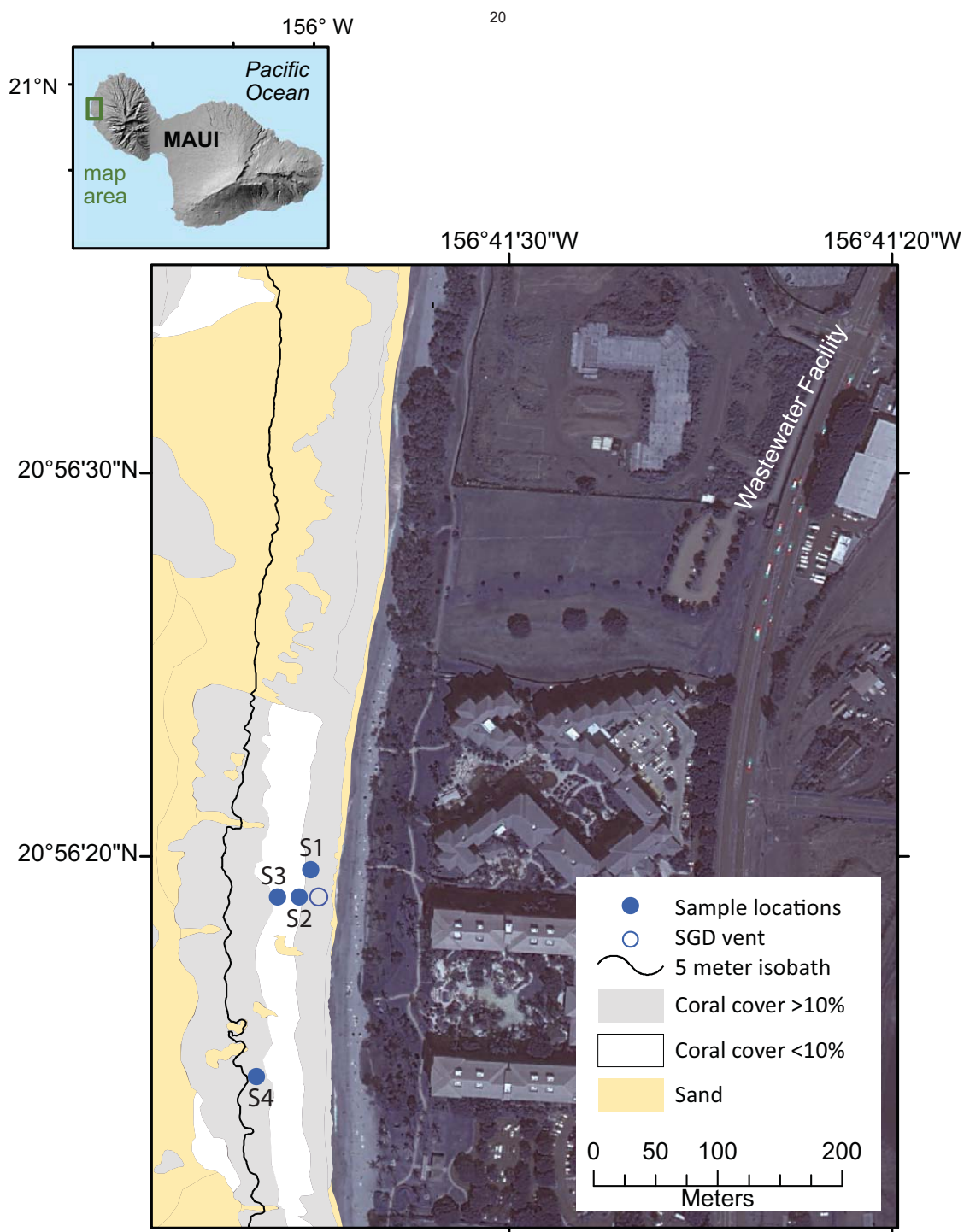




Figure 2

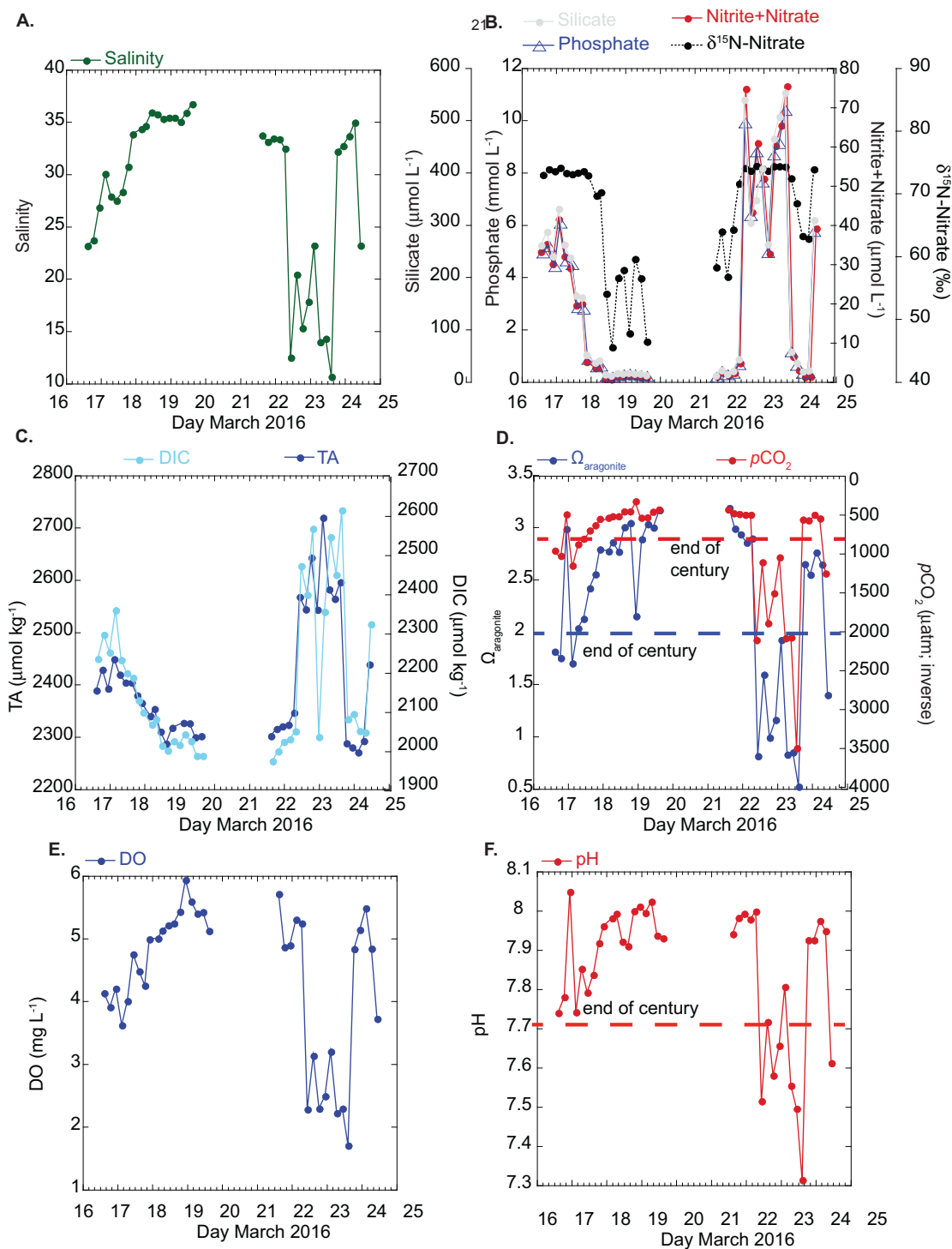




Figure 3

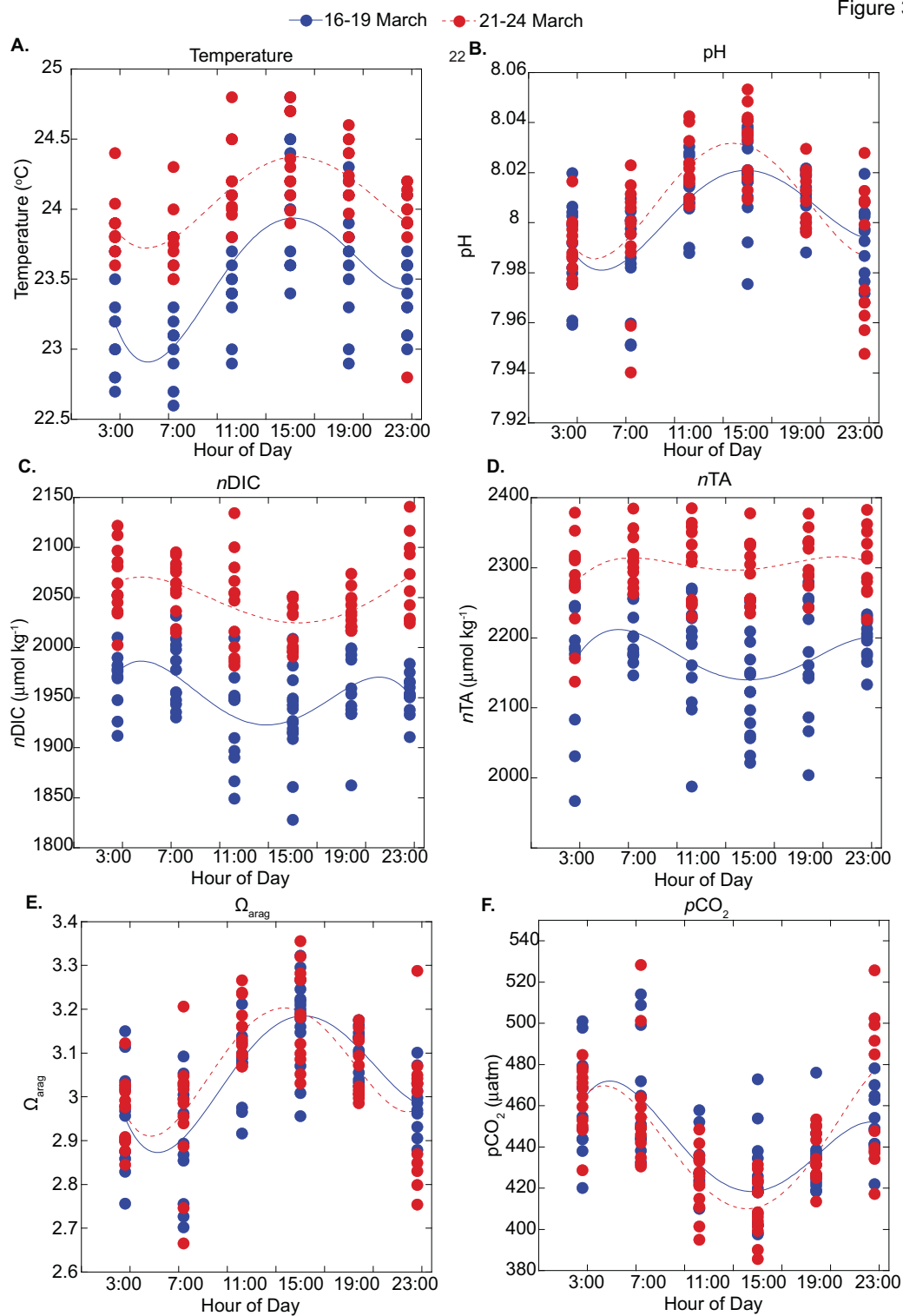




Figure 4

■ March 16-19, 2016  
■ March 21-24, 2016

